Ocean Engineering 155 (2018) 411–424

Contents lists available at ScienceDirect

Ocean Engineering

journal homepage: www.elsevier.com/locate/oceaneng

Assessing the performance durability of elastomeric moorings: Assembly investigations enhanced by sub-component tests

T. Gordelier [a,*], D. Parish [a], P.R. Thies [a], S. Weller [a], P. Davies [b], P.Y. Le Gac [b], L. Johanning [a]

[a] Renewable Energy Research Group, University of Exeter, Penryn Campus, Cornwall, UK
[b] IFREMER Marine Structures Laboratory, Centre de Brest, Plouzané, France

ARTICLE INFO

Keywords:
Marine energy
Mooring
Elastomer
Durability
EPDM
Component testing

ABSTRACT

The growing marine renewable energy sector has led to a demand for increasingly compliant mooring systems. In response, several innovative mooring tethers have been proposed demonstrating potential customisation to the stiffness profile and reduced peak mooring loads. Many of these novel systems utilise materials in a unique application within the challenging marine environment and their long term durability remains to be proven.

This paper presents a multifaceted investigation into the durability of a novel polyester mooring tether with an elastomeric core. Laboratory based functionality tests are repeated on tether assemblies following a 6 month sea deployment. Results show a 45% average increase in dynamic axial stiffness. This is supported by high tension laboratory based fatigue endurance tests showing a peak increase in dynamic axial stiffness of 42%. Sub-component material tests on the core elastomer support the assembly tests, separately demonstrating that certain aspects of tether operation lead to increased material sample stiffness. The average increase in material radial compressive stiffness is 22% and 15% as a result of marine ageing and repeated mechanical compression respectively; these are the first results of this type to be published.

The performance durability characterisation of the tether establishes the mooring design envelope for long-term deployment. This characterisation is crucial to ensure reliable and effective integration of novel mooring systems into offshore engineering projects.

1. Introduction

The highly dynamic nature of many marine renewable energy devices places new demands on mooring system design in contrast to conventional oil and gas floating offshore systems. In addition to reliably maintaining the station keeping of a device, for many device designs the mooring system must also provide the compliance required to harvest energy from the marine environment. Synthetic mooring ropes are now commonly used in this application (Weller et al., 2015a; Davies et al., 2014; Ridge et al., 2010) having greater compliance than wire rope or chain alternatives. For conventional synthetic ropes the compliance is correlated to the specified minimum breaking load (MBL). Hence, the compliance of the mooring system is frequently compromised in order to achieve the required MBL to survive the loads expected during operation. Additional compliance can be introduced through system architecture, utilising floats and weights in catenary mooring systems (Weller et al., 2014a). However, this introduces complexity, increases the risk of entanglement and increases the mooring footprint when ambitions for industry offshore deployments are striving for increasingly compact mooring footprints in array configurations.

As a response to these new demands, several innovative mooring systems have been proposed to introduce greater compliance into the mooring system, and in some cases, provide customisation to the stiffness profile of the mooring (Parish and Johanning, 2012; McEvoy, 2012; Bengtsson and Ekström, 2010; Luxmoore et al., 2016). Studies have shown these systems have the potential to reduce peak loads observed in the mooring system (Thies et al., 2015; McEvoy, 2012; Parish et al., 2017; Luxmoore et al., 2016). Thies et al. (2015) demonstrate a maximum line tension reduction of 20% and a mean line tension reduction of 10%, while McEvoy (2012) shows an 80–90% load reduction in a storm scenario when substituting conventional mooring configurations for a novel elastomeric tether. It is anticipated that a reduction in mooring loads will allow the down rating of other mooring components leading to a downward spiral of reduced weight and further reduced loads, with the potential to reduce the structural requirements and mass of the floating body (Parish et al., 2017). Estimates suggest foundations and mooring

* Corresponding author.
E-mail address: T.J.Gordelier@exeter.ac.uk (T. Gordelier).

https://doi.org/10.1016/j.oceaneng.2018.02.014
Received 18 August 2017; Received in revised form 20 December 2017; Accepted 4 February 2018
Available online 23 March 2018

Abbreviations

ACM	Axial Compression Modulus
DGPS	Differential Global Positioning System
DMaC	Dynamic Marine Component Test Facility
EPDM	Ethylene Propylene Diene Monomer
ETT	Exeter Tether Test series identifier
IFREMER	Institut Français de Recherché pour l'Exploitation de la Mer
IMU	Inertial Measurement Unit
ISO	International Organization for Standardization
MBL	Minimum Breaking Load
MTS	MTS Systems - manufacturer of testing equipment
NWBS	New Wet Breaking Strength
OCIMF	Oil Companies International Marine Forum
OPERA	Open Sea Operating Experience to Reduce Wave Energy Cost
RCS	Radial Compressive stiffness
SWMTF	South West Mooring Test Facility
TCLL	Thousand Cycle Load Limit

systems account for 10% of device costs (Low Carbon Innovation Coordination Group, 2012) and given the strong correlation between MBL and cost of mooring components (Harris et al., 2004), the potential savings through use of these novel systems are significant. Ultimately, the resulting mooring system will be lighter, cheaper and easier to deploy.

If these novel systems are to be successful, the long term performance must be proven and, given the harsh operating environment of marine renewable energy devices, this remains a key priority for these systems. The focus for the work presented here is a durability assessment of the Exeter Tether (Parish and Johanning, 2012), focusing on both the tether assembly and detailed material tests of the elastomeric core. The paper is organised into five parts. In this introduction the key features and operating principles of the tether are presented. Section 2, Methods, outlines the test facilities and techniques employed. Section 3, Results, presents key findings from the study followed by a Discussion in Section 4 which puts these results into the operating context of the tether and addresses the limitations of the work. Finally Section 5 details the conclusions and outlines next steps for this work.

1.1. The Exeter Tether

A detailed overview of the Exeter Tether and the P1 Prototype Series is presented in (Gordelier et al., 2015). A summary is provided here, based upon the specific prototype iteration utilising a core of seven solid elastomeric cords. The Exeter Tether comprises a hollow polyester rope braided around a core assembly of EPDM (Ethylene Propylene Diene Monomer) polymer strands wrapped in an anti-friction membrane as detailed in Fig. 1a. The polyester rope acts as the predominant load carrier and is terminated at either end with an eye splice.

The key principles of operation to appreciate are:

1. When under load, the tether extends along its length (axially) and simultaneously contracts across its diameter (diametrically), according to the helix angle of the braided rope.
2. As the rope diameter contracts, the elastomer core is compressed radially. The core resists this compression and thereby acts to resist the axial extension of the rope.
3. The compressibility of the elastomeric core dictates the resistance to diametric contraction, and in turn controls the axial extension. This compressibility is determined by both the cross-sectional form of the core and the material selection.
4. The helix angle of the braided rope dictates the ratio of the force vectors that act axially to extend the rope and circumferentially to compress the core. Typical helix angles for the P1 Prototype Series are detailed in (Gordelier et al., 2015).
5. Points (3) and (4) result in two distinct phases of tether extension as detailed in Fig. 2:
   (a) **Phase 1** - During the first phase of extension the elastomeric core strands are more easily deformed from seven individual round sections to eliminate the free space between the strands. At the same time, the helix angle is high, giving the braided rope considerable mechanical advantage in compressing the core. These factors combine to produce low axial stiffness during the first phase of extension.
   (b) **Phase 2** - As the free space in the core bundle tends towards zero, the resistance to further radial compression increases non-linearly. Simultaneously the extension of the tether also reduces the helix angle of the braid, thus reducing the rope's mechanical advantage over the core. These changes result in a second phase of extension which displays a marked increase in axial stiffness.

Critically, the choice of core geometry and material can be selected completely independently of the hollow rope. Thus, a series of tethers with the same MBL can be designed with a range of compliance values selected specifically for a device or location.

The working concept of the tether is presented in (Gordelier et al., 2015). This details the results from a *Proof of Concept* study with the P1 Series of 14 tether prototypes comprising a range of tether stiffness profiles achieved by varying the profile geometry and the Shore A hardness value of the elastomeric strands. The results presented in this paper focus on three of these tethers; the construction of these tethers is detailed in Table 1. It should be noted that the sheathing acts as an

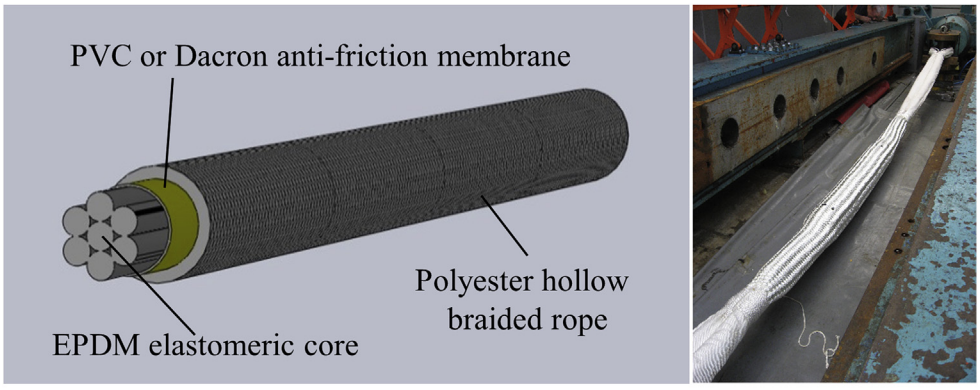

Fig. 1. The Exeter Tether. (a) Schematic detailing key components of P1 prototype series, replicated from (Gordelier et al., 2015); (b) full scale tether prototype from P4 series undergoing minimum breaking load testing at Lankhorst Ropes.

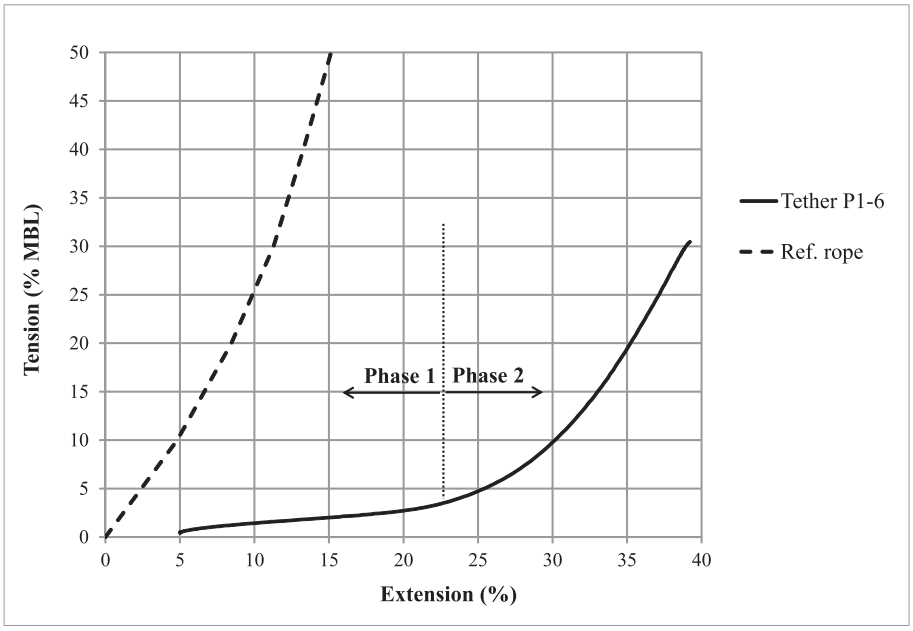

Fig. 2. Normalised stiffness profile for tether prototype P1-6 as established in (Gordelier et al., 2015), included here to demonstrate Phase 1 and 2 stiffness profiles. Reference rope included for comparison is a double braid polyester rope.

Table 1
Construction details of P1 tethers analysed in this paper. †Core comprises of 7 extruded profiles of specified cord diameter. *Core material of specified EPDM Shore A hardness from supplier (A) or (B). **Working length of tether which is the length of the EPDM core and does not include eye splices.

Prototype	Core cord diameter†	Core material*	Sheathing tape	Length**
P1-3	Ø25 mm	59A (A)	PVC	2.5m
P1-8	Ø25 mm	70A (B)	Dacron	2.5m
P1-16	Ø20 mm	70A (B)	PVC	2m

anti-friction membrane and to limit biofouling of the elastomeric core but will have minimal effect on the stiffness profile of the tether.

If the benefits of increased compliance offered by the Exeter Tether are to be realised, the long term performance of the tether must be understood. The work presented in this paper outlines an investigation into the evolution of the stiffness profile of the tether when subjected to both sea trials and high load fatigue testing. It compares functional tether assembly test results to material tests which include analyses of the effects of marine ageing and cyclic compression on the EPDM core material. This work is of critical importance to the ongoing development of the Exeter Tether, and is also of interest to other mooring developers utilising elastomers in their proposed novel mooring systems (McEvoy, 2012; Bengtsson and Ekström, 2010). Mooring designers looking to exploit novel mooring systems will be interested in these findings for improved understanding of long-term performance and to inform the correct specification of mooring system configurations utilising these novel solutions. Finally, establishing the impact of marine ageing and compression testing on EPDM will be of interest to anyone utilising this material in these or other relevant applications.

1.2. Research approach

The work presented in this paper details a combined approach utilising both assembly test techniques and sub-component material tests to investigate the durability of the elastomeric tether in the proposed operating environment. To provide an overview of the test approaches applied, Table 2 is included, which outlines the assembly and sub-component investigations completed. Each of the listed test procedures has a dedicated section in the Method, Results and Discussion chapters that follow.

Table 2
Research approach.

Test Work	Durability Aspect	Facility
Tether assembly tests		
Functionality tests following sea trials.	Marine ageing and operational loading of tether assembly.	SWMTF & DMaC
Tension-tension assembly fatigue tests.	High cycle number and high load fatigue testing of tether assembly.	DMaC
Sub-component material tests		
Establishing baseline EPDM material properties.	Baseline axial compression modulus and radial compressive stiffness.	IFREMER
Marine exposure investigation.	Effect of marine exposure on baseline EPDM material properties.	IFREMER
Radial compression fatigue investigation.	Effect of repeated compression cycles on baseline EPDM material properties.	IFREMER

2. Methods

The challenge for offshore technology innovations is validation during early development in order to demonstrate and eventually commercialise a novel concept. Whilst full-scale field tests are preferable and reduce potential scale-induced uncertainties (Mueller and Wallace, 2008), they are expensive and challenging to control. Laboratory based tests offer a high degree of control but can limit the scale and relevant factors that can be investigated (Salter, 2003).

This work has chosen a combined approach. Based on realistic, large-scale field test exposure, the operational durability of the tether is assessed. The assessment is further enhanced through repeated, controlled experimental tests at assembly and sub-component level. The performance durability appraisal can thus be based on both test methods.

This section initially describes facilities utilised before describing the test procedures adopted.

2.1. Test facilities

Tether prototypes were exposed to realistic operational conditions through deployment on a mooring limb of the South West Mooring Test Facility (SWMTF). This is an at-sea test facility located just inside the harbour limits of Falmouth Bay, Cornwall, UK. A fully autonomous instrumented buoy is configured to enable mooring components under

investigation to be deployed on mooring limbs and exposed to a typical mooring environment, with in-line and tri-axial load cells to monitor mooring loads. Further details of the facility are provided in (Johanning et al., 2008). For the purposes of this work, the SWMTF test facility was utilised to expose Exeter Tether prototypes to both marine ageing and simultaneous cyclical loading at typical mooring loads.

Controlled testing of the tether assembly was conducted in the Dynamic Marine Component Test Facility (DMaC). This facility provides fully submersible freshwater testing of components up to 6m in length and 0.8m diameter, with a 1m stroke linear hydraulic actuator able to deliver tension or compression forces of 30t dynamically and 45t statically. Further details of the test facility are available in (Johanning et al., 2010). The 444 kN pancake load cell controlling the linear actuator is calibrated annually and upon re-positioning; a full calibration was conducted in advance of this work and is reported in (Gordelier et al., 2015).

Material testing of the EPDM was conducted at the IFREMER[1] Marine Structures Laboratory. ISO7743 tests were conducted using an Instron 5566 load frame with a 10 kN load cell. Compression fatigue testing of the samples was conducted using an MTS test machine with a 250 kN load cell. Immersion of material samples in natural sea water was conducted using a bespoke system developed at IFREMER comprising a 60 L fresh seawater tank. The water was maintained at a constant temperature of 60 °C whilst being continually renewed with fresh sea water from the Brest estuary at a replacement rate of 60 L/24hrs. All equipment in the IFREMER laboratory is annually calibrated as part of the ISO9001 Quality Management Systems accreditation of the laboratory.

2.2. Assembly functionality tests following sea trials

Four prototype tethers were deployed on mooring limb 1 of the SWMTF from 4th June 2013 to 26th November 2013. Mooring limb 1 and mooring limb 3, installed at 185° and 65° respectively, experience the highest mooring loads due to the dominant wave conditions on the site as observed during previous deployments (Harnois et al., 2013, 2016). The composition of a typical SWMTF mooring limb is detailed by Harnois et al. in (Harnois et al., 2012). The existing 20m section of nylon rope at the top of the mooring line was replaced with four tethers; the focus for the work presented in this paper is tethers P1-3 and P1-8, with EPDM core Shore A hardness values of 59A and 70A respectively. P1-8 was situated at the top of the mooring line connected into the tri-axial load cell of the SWMTF via shackles. P1-3 was connected into P1-8 via a lanyard hitch. This top zone of the mooring line where P1-3 and P1-8 were located was anticipated to be the most aggressive zone for tether deployment.

A qualitative assessment of the tethers was conducted following the deployment to assess degradation of the tether and sub-components; this assessment is reported in (Gordelier et al., 2015). For the purposes of the work presented here, in order to quantitatively assess the change in dynamic axial stiffness of the tethers, the DMaC test facility was used to conduct tether functionality tests both before and after the six month sea deployment. Force driven conditioning tests were conducted, followed by a displacement driven test exercising the tether to a displacement of 0.9m for 5 cycles at an 8s period. The displacement of 0.9m was selected to maximise the extension available within the 1m stroke range of DMaC, and a cycle period of 8s was selected to represent a typical operating period. This is important due to the time dependant nature of the EPDM core material. The drive data for this test, ETT-08, are presented in (Gordelier et al., 2015) and the load-extension results from the fifth cycle of this test were extracted and processed to establish the stiffness profile of the tethers pre and post SWMTF deployment. The processing involved a deduction to account for the extension of the eye splices as measured and reported by (Gordelier et al., 2015). To account for the reduced eye splice extension following the sea deployment, an adjustment was made assuming that the extension of the eye splice reduces in accordance with a typical worked polyester rope. The Viking Braidline polyester rope was selected as the most appropriate reference rope, which over the full operating range demonstrates an average reduction in extension of approximately 25% upon working (Bridon, 2017).

Various approaches are suggested by (McKenna et al., 2000) to quantify axial stiffness and further alternative approaches are applied by (Davies et al., 2012), (Flory et al., 2004) and (ISO, 2007). In this assessment the secant modulus approach was adopted, utilising linear interpolation to calculate the exact strain at specified loads during load-up of the fifth cycle, and plotting the secant between these loads. To normalise this value it was divided by the tether MBL, as suggested by (Davies et al., 2002). Given the dynamic nature of these tests at 0.125 Hz, this non-dimensional parameter is termed dynamic axial stiffness, K_D.

Given the two distinct phases of tether stiffness as outlined in Section 1.1, K_D is quantified separately for each phase. During these basic functionality tests, the first phase was identified between a load of 5–10 kN and the second phase from 20 to 40 kN. Adapting the equations detailed in (ISO, 2007), the stiffness can be written numerically as:

$$K_{D,x\rightarrow y} = \frac{(F_y - F_x)/(F_{MBS})}{\varepsilon_y - \varepsilon_x} \quad (1)$$

Where $K_{D,x\rightarrow y}$ is the dynamic axial stiffness between loads x and y, F_x and F_y are the loads at x and y respectively, F_{MBS} is the minimum breaking load of the sample and ε_x and ε_y are the calculated strains at x and y respectively.

This approach was repeated for tether prototypes P1-3 and P1-8 before and after the SWMTF deployment.

Further to the assessment of the tether stiffness profile, it was originally anticipated that an assessment of load data from the 69 kN axial load cells and 69 kN tri-axial load cells located at the top of each mooring line would allow for a quantitative assessment of the impact of the mooring tether on mooring loads and additionally log the load exposure profile of the tethers during the deployment. However, the load cells failed early during this deployment. Numerical modelling to estimate mooring loads utilising data collected from the SWMTF inertial measurement unit (IMU) and digital global positioning system (DGPS) is ongoing and will be the subject of future publications. Typical load profiles for SWMTF mooring limbs during previous deployments are detailed by (Harnois et al., 2016) and demonstrate peak mooring loads for Limb 1 exceeding 50 kN with typical operational mooring loads below 10 kN and typical peak periods ranging from 2 to 11 s.

2.3. Tension-tension assembly fatigue tests

To establish a fatigue performance benchmark for the P1 Series a *Thousand Cycle Load Limit* (TCLL) test was conducted. This test, designed by the Oil Company's International Marine Forum (OCIMF), was established to quantify mooring hawser response to tension-tension fatigue (Oil Companies International Marine Forum, 2000). The test subjects the component to a series of 1000 tension cycles at increasing load levels; starting with 50% NWBS (new wet breaking strength) and increasing in 10% increments until the sample fails. The test is conducted with the tether fully submerged in fresh water. Full details of the test method, establishing the NWBS of the tether (222 kN) and the full calculation of the TCLL value for the tether are presented in (Gordelier et al., 2015).

Of specific interest to the work presented here is the stiffness performance of the tether. The TCLL test was therefore analysed to quantify the evolution in dynamic axial stiffness of the tether throughout the TCLL testing series. The test failed during cycling at 70% NWBS so there is a full data set of 1000 cycles at 50% and 60% NWBS load levels, and a partial set of data available at 70% NWBS load level (the sample failed on 176th cycle of the 70% level).

The tether utilised for the TCLL test was P1-16; this is a modified tether, with a reduced working length to enable the high extensions of

[1] Institut Français de Recherché pour l'Exploitation de la Mer.

the TCLL test to be achieved within the working constraints of DMaC. The tether core is manufactured from seven Ø20 mm 70 Shore A EPDM strands from supplier B. Due to the different construction of this tether, it is not possible to directly compare the results to those from the field test at the SWMTF. The results however, do provide useful insight into the evolving stiffness profile of the tether design concept when worked at high loads.

The secant modulus approach was again adopted here as one of the standard approaches suggested by (McKenna et al., 2000). Again, to reflect the two distinct phases of tether operation K_D was calculated separately for each phase. Due to the different tether construction and test parameters, the load values identified to represent the two phases of tether operation were updated for these fatigue tests, with the Phase 1 secant from 10 to 30 kN and the Phase 2 secant from 60 to 100 kN. Selecting 100 kN as the peak value for the secant ensured a consistent approach was applied between load levels as a full secant could be captured even at the lowest load level, which peaked at 110 kN. The dynamic stiffness was calculated at a range of cycle numbers throughout the TCLL test. At each cycle of interest, the data was linearly interpolated to calculate the exact strain at the specified load level, and utilising Equation (1) the dynamic stiffness, K_D, was calculated.

2.4. Sub-component EPDM material tests

2.4.1. Establishing baseline material properties

A key principal of the tether is the control of axial stiffness by varying the core material and construction, with each core configuration providing a particular resistance to compression. The compression stress-strain properties of the core material are therefore critical to the operation of the tether; understanding how these material properties might be affected by ageing of the core material, or exposure to multiple compression fatigue cycles is important for ascertaining long term performance. ISO7743:2011 *Rubber, vulcanized or thermoplastic determination of compression stress strain properties* (ISO, 2011) provides a standard to calculate the compression modulus of a given polymer. Quantifying this property for virgin material can then be used as a benchmark to compare with further material tests following marine ageing or compression fatigue exposure. It should be noted the ISO7743 test is conducted in air.

2.4.1.1. Axial compression modulus. The ISO7743 test procedure was followed to subject a cylinder of material to axial compression at a rate of 10 mm/min to induce a strain of 0.25. The load was then removed at the same rate. This was repeated to give four compression cycles in total. Data from the fourth cycle was used to calculate the compression modulus at a strain of 0.1 and 0.2 using Equation (2).

$$E_{c,x} = \frac{\sigma_x}{\varepsilon_x} \tag{2}$$

Where $E_{c,x}$ is the compression modulus at strain x (in MPa), σ_x is the stress at strain x which is calculated by $\frac{F_x}{A_o}$ (in MPa), ε_x is the strain at x which is calculated by $\frac{L_x - L_o}{L_o}$, F_x is the load at strain x (N), A_o is the original area (mm^2), L_x is the length at strain x (mm) and L_o is the original length (mm).

The ISO standard provides a choice of test pieces and methods. The results presented here are based on the procedure standard reference Test Piece B (Fig. 3a), Method C[2] As the EPDM material was supplied in 25 mm extruded section, and the compression modulus is affected by both the material properties and the manufacturing process, the standard Test Piece B dimensions were scaled up, so that the test could be conducted on the 25 mm section; these dimensions are detailed in Fig. 3b. Results from these tests, compressing the sample axially (along the axis of the extruded EPDM), are referred to as the Axial Compression Modulus (ACM). For each test condition, three separate samples were tested.

2.4.1.2. Radial compressive stiffness. In addition to the ACM tests, of specific interest to the operation of the tether is the compressibility of the EPDM across the diameter of the cord. This is not a standard ISO test and, unlike the ACM tests, the cross section of the sample in the radial direction is not consistent and the stiffness in this direction is related to both the material and the geometry of the sample. As this is not a standard test it is not comparable to external sources, however, quantifying the stiffness of the sample in this direction allows for a direct comparison across the range of EPDM hardness values and an understanding of how fatigue compression exposure and marine ageing of the material affect this crucial property. The same procedure was followed as outlined for ACM. As this is not a direct calculation of material modulus, this result is referred to as the Radial Compressive Stiffness (RCS). The target dimensions for the RCS samples are detailed in Fig. 3c. It should be noted that in some of the extruded EPDM sections a 2–3 mm flat ridge was evident running along the length of the cord; this was a product of the manufacturing extrusion process. To minimise the effect of this ridge the sample was orientated ensuring the ridge was at the side and the sample was marked with a white dot to ensure consistency between sample measurements and test procedures.

Three repeat tests were performed for both ACM and RCS across the range of Shore A hardness values specified: 54, 59, 70, 70.7 and 80.7. The durability aspect of this work was to ascertain whether these properties are affected by the operational requirements of the tether and a mid-range EPDM with Shore A hardness 70.7 was selected for further testing as detailed below.

2.4.2. Marine exposure investigation

In operation, the Exeter Tether will be submerged in the marine environment for extended periods of time. At the time of writing there is no published data regarding the stability of EPDM in a submerged marine environment and this information is critical to establishing the marine durability of this elastomeric tether in service. In a limited test window, a widely used approach to accelerate the effect of polymer ageing in a marine environment is to immerse samples in heated sea water. There is a significant amount of literature detailing the use of this approach for ageing polymers (Celina et al., 2005; Gillen et al., 2005; Le Gac et al., 2012; Le Saux et al., 2014; Scheirs, 2000; Wise et al., 1995). A linear Arrhenius extrapolation is generally used to relate the accelerated ageing conducted at elevated temperatures and extrapolate this to estimate the effects of longer term ageing at lower temperatures. This relationship relates reaction rate to time and temperature through the relationship detailed in Equation (3) (Celina et al., 2005).

$$k = A \times e^{\frac{-E_a}{RT}} \tag{3}$$

Where k is the reaction rate, A is the pre-exponential factor, E_a is the Arrhenius activation energy, R is the gas constant (8.314 J/mol.K) and T is the temperature (in K).

From Equation (3), the natural logarithm of reaction rate k can be related to the inverse of temperature $\frac{1}{T}$ via a linear relationship. As detailed by (Celina et al., 2005) degradation time t is related to reaction rate by $\frac{1}{k}$. To date, there are no data available for the specific effect of marine ageing at an elevated temperature on EPDM. Based on previous work ageing polymers (Le Gac et al., 2012), 60 °C was selected as an appropriate temperature to speed up the ageing process but minimise oxidation of the EPDM, which could result in excessive deterioration of the material.

EPDM samples were cut to the dimensions detailed in Fig. 3c and

[2] Four methods are listed A-D in the standard. Method C specifies the sample can be lubricated or not lubricated, and compressed at a speed of 10 mm/min to a strain of 0.25 for four uninterrupted cycles. Refer to (ISO, 2004) for full details.

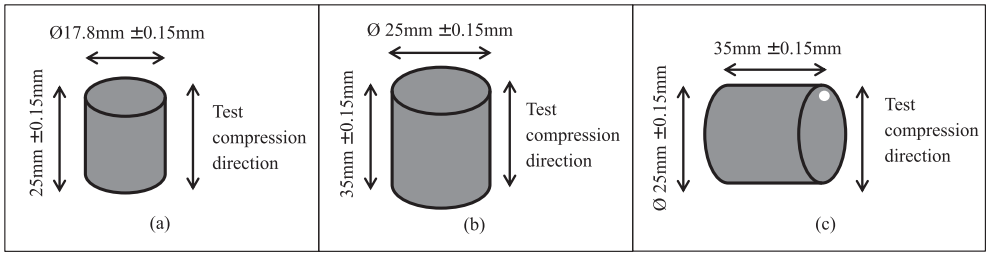

Fig. 3. ISO7743 sample target dimensions. (a) As specified for Test Piece B; (b) scaled up to suit the Ø25 mm extruded section; (c) Radial compressive stiffness test dimensions, white dot to aid sample orientation and avoid flat ridge. (Images not to scale.)

immersed in natural sea water tanks as detailed in Section 2.1, heated to a temperature of 60 °C for a period approaching 13 months (15/05/2014–10/06/2015). Regular weight measurements were recorded to monitor sample saturation. Immediately following removal from tanks the ISO7743 test procedure was conducted as detailed in Section 2.4.1 to establish the RCS following marine ageing.

2.4.3. Radial compression fatigue investigation

During operation the tether extends and contracts to accommodate the wave induced motion of a floating body. This in turn exposes the EPDM core to repeated radial compression and axial extension cycles. This is a durability concern for the tether as the long term consequence of these actions is unknown. To investigate the potential effects of this process, samples of the EPDM core were subjected to repeated compression cycles and the ISO7743 procedure was used to calculate the RCS of the sample following this exposure.

Material samples were prepared to the dimensions detailed in Fig. 3c and set up in the MTS compression test machine using a 250 kN load cell. A small dot of cyanoacrylate was used to secure the underside of the cord to the MTS load platen as during trials the sample had been observed slipping out of the test machine. A compromise was required in specifying a frequency that maximises the number of cycles in a given test window whilst limiting the self-heating of the sample. A preliminary investigation into the test parameters using an infra-red camera indicated that at a compressive diametral strain of 0.2 the frequency of compression cycles should be limited to 2 Hz. Frequencies greater than this led to excessive self-heating of the EPDM sample, with surface temperatures beyond 10 °C. The MTS machine was set to operate in displacement mode, with a diametral strain of 0.2 calculated from the average of three measurements of the cord diameter.

The test sample was subjected to 707,000 compression cycles to a strain of 0.2 and a frequency of 2 Hz. The RCS test procedure (outlined in Section 2.4.1) was conducted immediately following the compressive testing and at subsequent intervals to observe any time dependency in the results. Conducting the ISO test both radially and axially on one single sample was not considered good practice as one procedure may affect the other and, as the critical property of interest in this instance was the radial compressive stiffness, the test was only conducted radially.

3. Results

3.1. Assembly functionality tests following sea trials

Following a sea deployment approaching 6 months, processed data from the fifth load up cycle of DMaC functionality test ETT-08 is detailed in Fig. 4. The secant for each line is identified in this figure between 5 and 10 kN for Phase 1 and from 20 to 40 kN for Phase 2. The calculated values for K_D are also identified for both virgin and worked samples. Table 3 presents the calculated increase in dynamic stiffness observed following the SWMTF deployment for each phase of operation.

Key observations from this assessment are a measurable increase in dynamic stiffness of the tethers following the sea deployment. The majority of the increase in stiffness is observed in Phase 1 of operation with an increase of 54% and 110% for tethers P1-3 and P1-8 respectively. Additionally, and perhaps more critically, the stiffness profiles of the worked tethers have become more aligned, settling on a similar stiffness profile as highlighted by Fig. 4. Pre-deployment during Phase 1, P1-3

Table 3
Calculated change in stiffness for Phase 1 and Phase 2 of tether operation following SWMTF deployment.

Tether	Change in stiffness	
	Phase 1	Phase 2
P1-3	+54%	+1%
P1-8	+110%	+15%

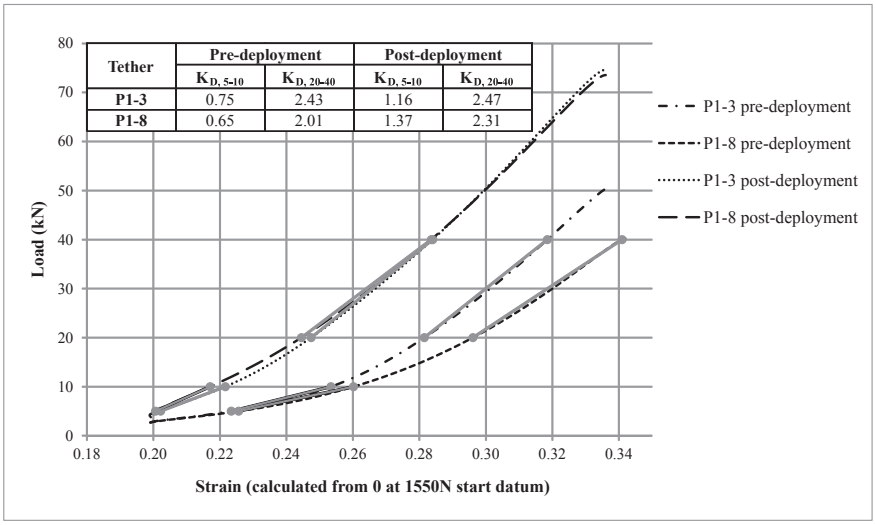

Fig. 4. Processed data from fifth load up cycle of functionality test ETT-08 for tethers P1-3 and P1-8 pre and post SWMTF deployment. Secant and K_D detailed for two phases of operation. Note strain measurement is from a displacement of 0 at a test start datum load of 1550N.

demonstrated a stiffness 13% greater than P1-8, however, following deployment the stiffness during this phase was 15% less than P1-8. During Phase 2 the difference in stiffness between P1-3 and P1-8 dropped from 17% to 6% following deployment. Given the design philosophy behind the tether is to establish a range of stiffness profiles, this finding is very relevant and will be further addressed in the Discussion, Section 4.

3.2. Tension-tension assembly fatigue tests

Data from the TCLL test is analysed to establish the evolution in dynamic axial stiffness of the tether throughout the test. An example of the approach is detailed in Fig. 5, which highlights the analysis for the 1–50% load level and details the secants established for the calculation of K_D. To complement this graph, Table 4 details the calculated value of K_D at each cycle and the % change in stiffness from cycle 5. During the 1–50% load level there is an initial period of high increase in dynamic stiffness; during the first 250 cycles there is an increase of 11% and 33% for Phase 1 and Phase 2 behaviour respectively. For Phase 1 the stiffness stabilises and from cycles 250–950 the stiffness increases by a further 3% whilst Phase 2 stiffness increases by a further 10%. During the last 250 cycles of this range the maximum increase is just 1% in both phases.

The same procedure was repeated for the 1–60% load level and the 1–70% load level. Fig. 6 provides a summary for the complete TCLL test series, capturing the dynamic axial stiffness calculated from the secants of Phase 1 and Phase 2 at cycles selected from all load levels. Plotting the data in this way highlights that the dominant change in stiffness during this high load fatigue test occurs in Phase 2 of the tether operation, where the functionality is dominated by the polyester rope rather than the EPDM core. The drop in stiffness observed between TCLL load levels is the result of adjustments required for the test set-up to accommodate recovery of the tether between load levels. Following completion of one load level the test ends at a load of 1% NWBS, however, as the tether recovers it attempts to contract in length. As it is fixed in the test machine, the result of this is an increase in load. To obtain a starting load of 1% NWBS for the subsequent load level, slack must therefore be introduced into the system, which results in the decrease in stiffness observed between the TCLL loading levels.

The results in Fig. 6 also show a small reduction in stiffness occurring in Phase 2 at the start of the 1–60% load level. This could be due to the higher load level causing local damage in the rope construction or slippage within the tether construction where the hollow braided rope slips off the tether core. Following this initial drop however, a steady increase in stiffness is observed, though less pronounced than the 1–50% range with a maximum increase of 6% over the full 1000 cycles. The stiffness again stabilises at higher cycle numbers. Results from the final load level of 1–70% demonstrate the gradual reduction in tether stiffness in Phase 2 as the polyester rope yields further and approaches final failure.

Table 4
Calculated value of K_D for each phase of stiffness at selected cycle number for the 1–50% load level. % change represents % increase in stiffness from a baseline at 5 cycles.

Cycle No.	1st phase secant		2nd phase secant	
	$K_{D,10-30}$	% change	$K_{D,60-100}$	% change
5	3.27	n/a	6.49	n/a
25	3.37	+3%	7.10	+9%
50	3.43	+5%	7.47	+15%
250	3.63	+11%	8.56	+32%
500	3.70	+13%	9.00	+39%
750	3.73	+14%	9.15	+41%
950	3.73	+14%	9.23	+42%

3.3. Sub-component EPDM material tests

3.3.1. Establishing baseline material properties

A typical load-strain plot from the ISO7743 test procedure is detailed in Fig. 7. The plot reveals the full extent of the Mullins effect that is observed in elastomers. It is characterised by the permanent softening of the stress-strain curve observed the first time a polymer is exposed to a compression or tension load (Cantournet et al., 2009). This can be seen in Fig. 7, where cycle 1 requires a greater load than any subsequent cycles. Utilising data from the fourth load cycle for the ISO calculations ensures the Mullins effect does not distort the results. Although this effect is clearly observable during the ISO7742 tests, the impact of this softening is minimal in comparison to the effects from marine exposure and radial compression of the material samples.

In line with the ISO standard, the fourth data cycle for each test run is extracted and good repeatability is observed between the repeat tests for each sample condition. The ACM or RCS is calculated at both 0.1 and 0.2 strain using Equation (2). It should be noted that the 0 strain point is determined from the point at which the curve of the last cycle meets the strain axis (where Force = 0N). This point is referred to as 'relative 0 strain' as it is not the absolute strain value. Linear interpolation is again used to extract the exact values at the required points. Where applicable, the average and standard deviation of each data set is calculated and the results can be seen in chart form in Fig. 8.

As expected, a positive correlation can be seen between Shore A hardness and the calculated values for ACM and RCS. The observed range

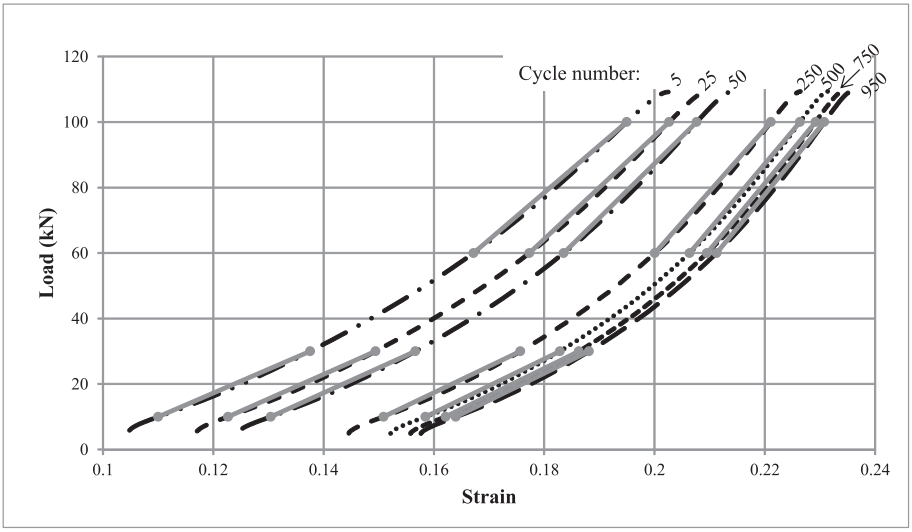

Fig. 5. Extracted data for selected cycle numbers for 1–50% load level of TCLL test for tether P1-16, conducted in fresh water. Secants identified between 10 and 30 kN for Phase 1, and 60–100 kN for Phase 2.

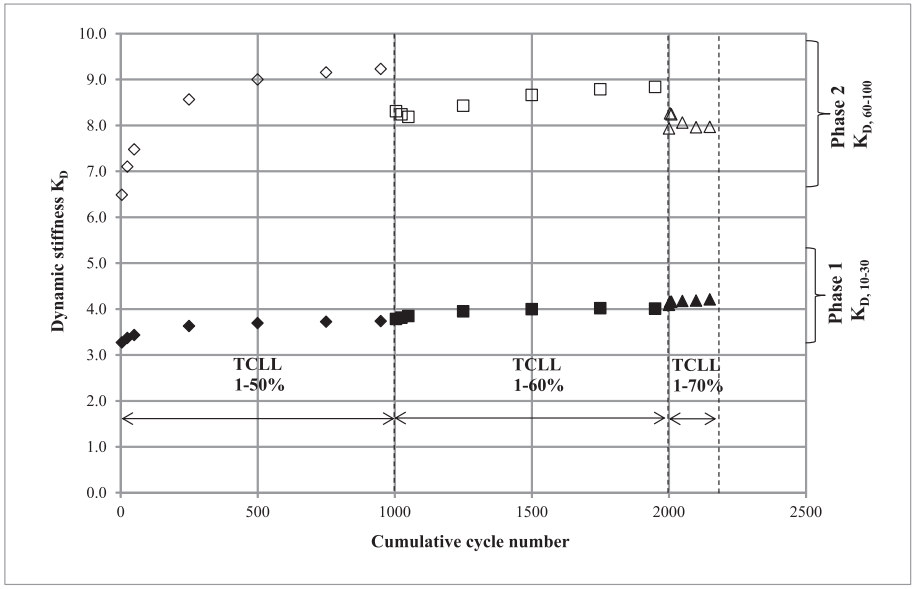

Fig. 6. Dynamic axial stiffness values calculated for selected cycles plotted against cumulative cycle number for all load levels of TCLL test for tether P1-16, conducted in fresh water. Note that short test breaks between TCLL load levels resulted in sample recovery which results in the observed drop in K_D between consecutive load levels.

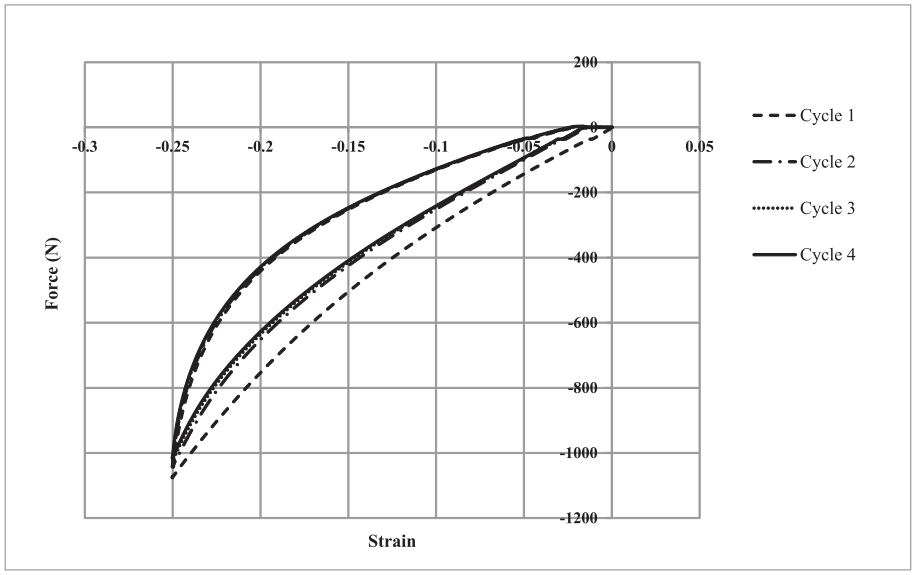

Fig. 7. ISO7743 full data set for sample 70–1 representing EPDM with 70.7 Shore A hardness, compressed radially. Note due to the compressive nature of these tests both force and strain are negative.

of stiffness values are a dominant factor controlling the variety of stiffness profiles observed in the tether assembly.

It is also evident that at each Shore A Hardness value the ACM and RCS calculated at a strain of 0.2 is always higher than that calculated at a strain of 0.1. Again, this is intuitively expected; at the higher strain level of 0.2 the sample is under greater compression and it will therefore demonstrate increased resistance to any further compression (and thus a higher result for ACM or RCS).

Having established baseline values of ACM and RCS across a range of Shore A hardness values, a mid-range EPDM material (Shore A hardness 70.7) was selected for a detailed analysis of the effect of marine ageing and fatigue compression cycles on key material properties. These results are presented in the next section.

3.3.2. *Marine exposure investigation*

During the marine exposure testing, samples were periodically removed for weighing to observe the saturation of the samples. It was anticipated that the weight of the samples would stabilise over time, once fully saturated. At 13 months, although the rate had slowed, a small amount of weight gain was still occurring (Fig. 9). Due to time limitations however, the samples were removed at this point for testing.

Following removal from the heated water the ISO7743 test was repeated on the aged samples of EPDM. Again the procedure was repeated on three samples from each range and Fig. 10 details the average and standard deviation of these samples in comparison with the virgin material.

The ageing process has significantly increased the material resistance to compression with ACM increasing by 14% and 16% at strains of 0.1 and 0.2 respectively, whilst RCS increased by 22% at both values of strain. Given the compression of the EPDM core is a significant factor controlling the stiffness profile of the operating tether assembly as detailed in (Gordelier et al., 2015) this finding has significant implications for the operation of the tether which will be further explored in the Discussion.

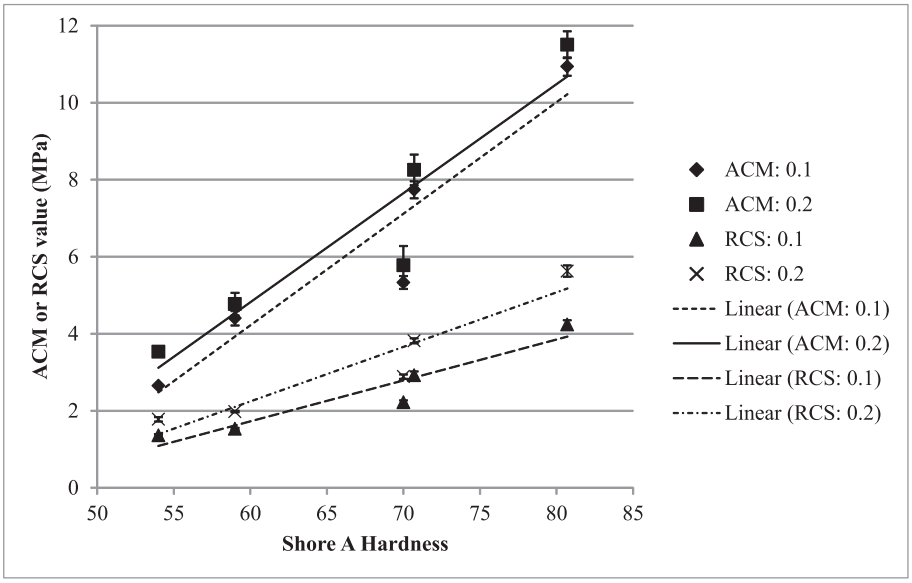

Fig. 8. ISO7743 axial compression modulus and radial compressive stiffness results for a range of EPDM Shore A Hardness materials, calculated at 0.1 and 0.2 strain. Where applicable, error bars represent sample standard deviation.

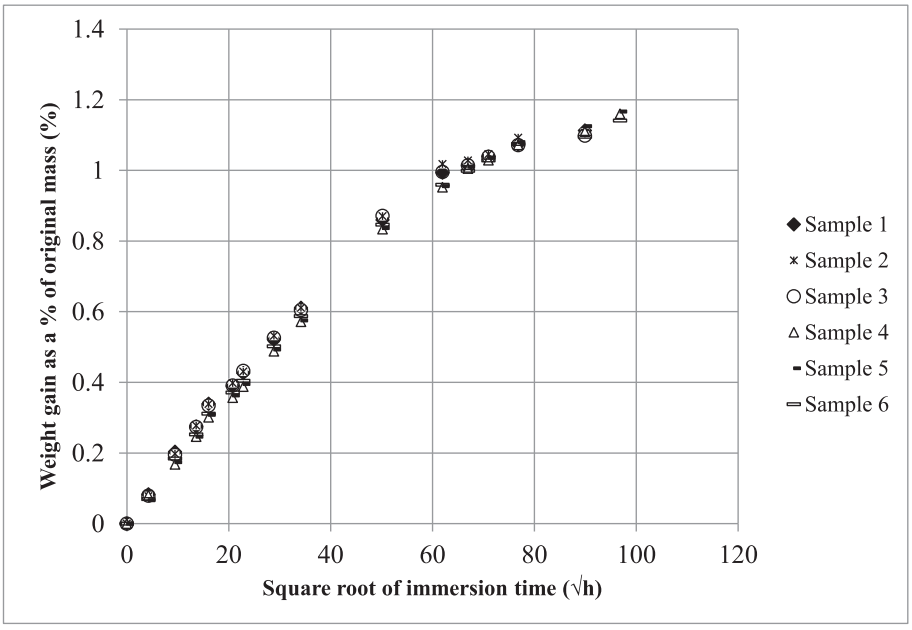

Fig. 9. Weight gain of 70.7 Shore A hardness EPDM samples based on Fig. 3c dimensions. Individual samples difficult to distinguish but general trend is apparent.

3.3.3. *Radial compression fatigue investigation*

RCS results calculated using the ISO7743 approach following 707,000 compression cycles at a strain of 0.2 and a frequency of 2 Hz can be seen in Fig. 11.

These results show that the immediate RCS of the sample, measured 12 min after the compression cycles, does not reflect the ultimate RCS once the sample has had time to recover. At the 12 min point, there is not a consistent change for RCS measured at 0.1 and 0.2 strain; at a strain of 0.1 RCS is 7% less than the control sample whilst at a strain of 0.2 it is 11% higher. Over time this difference diminishes; at 42h20 the RCS is 13% and 15% higher than the average control at strains of 0.1 and 0.2 respectively. ISO7743 is finally repeated 66h20 after the compression cycling, and provides RCS values 14% and 16% higher than the average control at strains of 0.1 and 0.2 respectively. Ultimately, these results show that exposure to extended compression cycling, at a strain of 0.2, can lead to a 15% average increased resistance to compression, in comparison to the un-fatigued control sample.

4. Discussion

4.1. *Assembly functionality tests following sea trials*

On comparing the observed increase in tether stiffness following the sea deployment to the expected performance for a conventional fibre rope, the literature is inconclusive. Although different methods have been applied, Weller et al. (2015b) review the performance of a nylon seven parallel-stranded rope and suggest a decrease in axial stiffness following an 18 month deployment at the SWMTF; this change in performance is attributed to mild internal abrasion damage occurring in the rope construction due to yarn on yarn wear, accelerated by the ingress of particulate matter including biofouling, during deployment. This result is of interest in the context of synthetic ropes, however, it is not directly

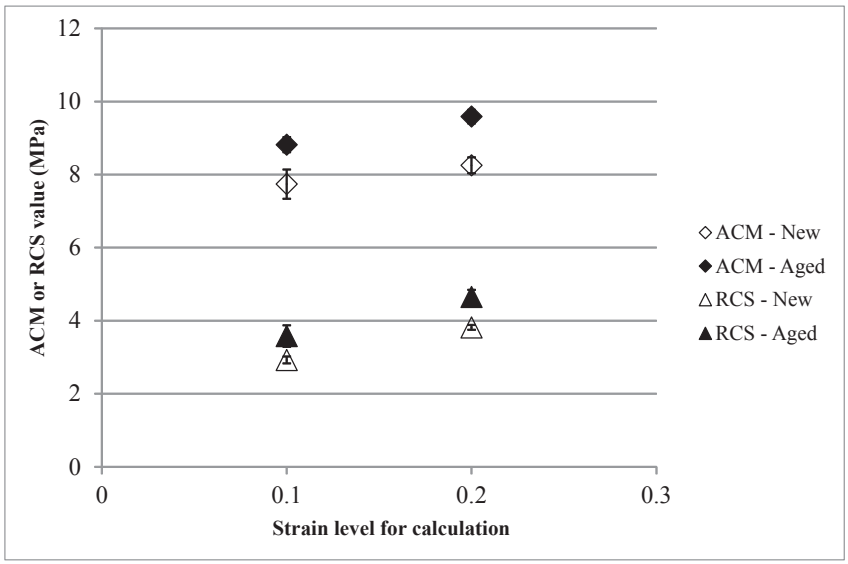

Fig. 10. Average ISO7743 results for ACM and RCS of new and aged EPDM 70.7 Shore A hardness. Error bars based on sample standard deviation.

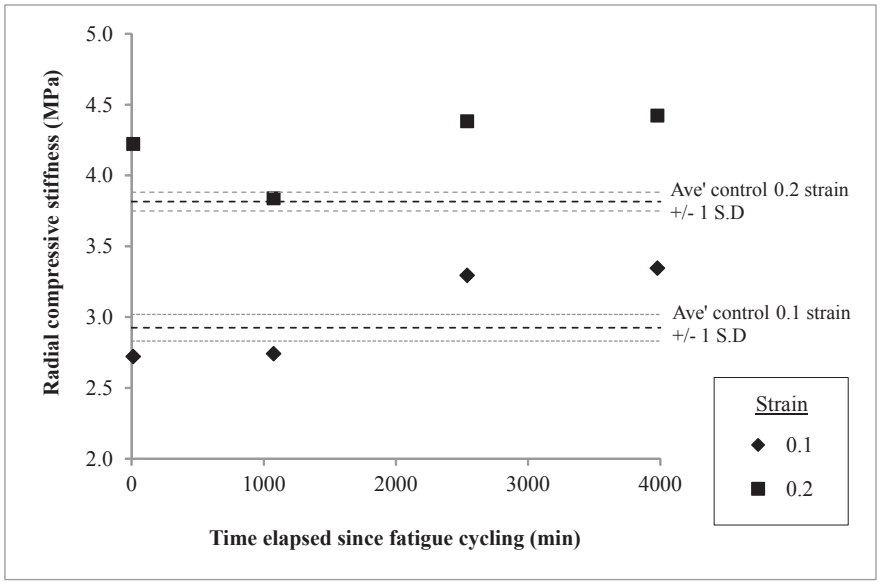

Fig. 11. Radial compressive stiffness values calculated using ISO7743 at intervals following compression fatigue cycling of 70.7 Shore A hardness sample of EPDM for 707,000 cycles at 20% compression and a frequency of 2 Hz. Control sample plotted for comparison, this was not subject to fatigue cycles.

comparable to the tether polyester rope.

The finding from (Weller et al., 2015b) is in contrast with results presented by (Bitting, 1980a) who observes an increase in axial stiffness for both nylon and polyester ropes when exposed to the ocean environment for 4–5 years. The polyester rope investigated is 8-strand plaited and double braided in construction and the dynamic stiffness increases 10–25% following the sea exposure. Further to this, data published by rope manufacturers generally indicate an increase in stiffness for worked ropes, with separate performance curves provided for new and worked ropes to inform system design. Typical worked graphs are published by rope manufacturer Bridon (Bridon, 2017) and demonstrate an average increase in stiffness of approximately 25% over the working range of a worked polyester rope (although the precise definition of 'worked' is not specified). Rope construction and material selection will significantly effect the change in stiffness observed, but overall it is anticipated that in the short to medium term synthetic ropes will get stiffer with use. As noted by (Weller et al., 2015b) a reduction in stiffness will be observed as the rope approaches failure, particularly if the failure mechanism is fatigue.

Given the changes observed in the stiffness profiles of worked conventional mooring ropes it is unsurprising to observe a change to the operating profile of the Exeter Tether prototypes following sea deployment, as the outer load carrying jacket is a hollow braided polyester rope. It is interesting to note however, that the dominant change in the stiffness of the worked tethers following sea deployment occurs during Phase 1 of operation which is dominated by the compression of the EPDM core, as outlined in Section 1.1. The average increase in stiffness following deployment of both tethers for Phase 1 is 82% in contrast to Phase 2 with an average increase of 8%. During the Exeter Tether operation, although Phase 1 is dominated by the EPDM core material properties, the increase in stiffness of the load carrying polyester rope will have an impact on tether operation across both Phase 1 and Phase 2.

The design concept of the P1 tether series utilises a standard braided rope jacket with a range of different polymer core specifications to achieve a variety of axial stiffness responses as demonstrated in (Gordelier et al., 2015). Therefore of interest, is the observed reduction in operating range of the post deployment tethers, given achieving this stiffness range was one of the key design intentions for the P1 Tether

Series. Results from EPDM material testing indicate an increase in stiffness of the EPDM material which would certainly lead to an alteration in overall tether stiffness profile. These results are discussed in more detail in Sections 4.3 and 4.4.

Of relevance to these tether assembly tests and the controlled assembly fatigue tests discussed in the next section, is the stiffness of standard polyester mooring lines and this behaviour in relation to average load and load amplitude. Expanding upon earlier work by (Bitting et al., 1980b), investigations with a 12 strand, parallel laid polyester rope presented by (Fernandes et al., 1999) demonstrate there is an increase in stiffness proportional to the average load applied, and a decrease in stiffness proportional to the load amplitude, with a limited effect from loading frequency. This work has been confirmed and further developed by (Davies et al., 2002) who also demonstrate a stiffness dependence on mean load and load range for both aramid and HMPE ropes. These observations are further supported by (Weller et al., 2014b) and (Weller et al., 2015b). To establish the change in tether stiffness observed pre and post SWMTF deployment, identical functionality test ETT-08 was repeated. This is a displacement driven test so small variations in the peak load of the fifth cycle are observable. However, the stiffness profiles are calculated at consistent loads for each sample, 5–10 kN for Phase 1 and 20–40 kN for Phase 2. Comparing the stiffness profiles in this respect should minimise the variation brought about by an increase in average load.

The main limitation of the tether assembly test work is due to the limited number of samples available and the large investment required for sea deployments. With the high costs involved at the early stage of prototype development, the total number of tethers manufactured for the P1 Series was limited to 13 and no two tethers were identical. Given the scope of test work required from this first set of prototypes it was not possible to conduct repeat sea tests on multiple samples. Results should therefore be considered to give an indication of performance trends rather than definitive values for stiffness profiles.

4.2. Tension-tension assembly fatigue tests

The TCLL fatigue endurance tests, performed in fresh water, highlight the increase in dynamic axial stiffness of the tether when subject to high load fatigue cycling. In addition to the increase of the individual cycle dynamic stiffness, an overall increase in sample length is measured. This extension is observed in conventional fibre ropes and is due to both the permanent bedding in of the rope and end terminations (material and constructional reorientation and stretch), creep and visco-elastic stretch which are accumulated during tension cycles (Flory et al., 2004). Work conducted on polyester fibres attributes an element of both the permanent and recoverable strain to the macromolecular rearrangement of entanglements and orientation of crystallites (Chailleux and Davies, 2005). Further to this (Davies et al., 2000), state that the majority of permanent bedding in strain is due to the material behaviour and not the rope construction for long lay length polyester mooring lines. Indeed the extent of the permanent stretch in polyester mooring ropes leads to a common practice of pre-stretching ropes during installation to minimise future adjustments required to the mooring system (DeAndrade and Duggal, 2010).

Regarding the recoverable element of the strain, in conventional fibre rope testing recovery of the accumulated elastic stretch and visco-elastic stretch is anticipated when the tension cycles stop. However in the tether, the time dependency of this recovery is particularly pronounced due to the additional recovery of the EPDM core which takes on a temporary compression set during cyclical loading. To accommodate this recovery, adjustments to the DMaC set-up led to a perceived drop in axial stiffness as observed between load level cycles detailed in Fig. 6. The significance of the observed compression set is caused by the high loading levels used in the TCLL test (up to 70% MBL in this case). Critics of the TCLL test procedure claim the high loading levels render it unrepresentative of the final application (Davies et al., 2012); certainly this time dependant recovery would be much less perceptible at the typical operating range of the tether. It should also be noted that the high level of loading in the TCLL test procedure accelerates any wear mechanisms occurring. The reduction in stiffness and final failure of the tether observed at the end of the TCLL test in Fig. 6 would be more gradual under typical operating conditions.

Weller et al. (2014b) analysed the performance of a conventional nylon rope with a parallel stranded sub-rope construction during cyclical loading and found that the axial stiffness stabilises from 25 cycles. In comparison to the results for the tether, significant evolution is still occurring at 25 cycles which suggests that due to the novel construction of the tether, establishing a stabilised axial stiffness profile during cyclical loading may take longer than for conventional fibre ropes. It should be noted however that the TCLL test presented here subjected the tether to significantly higher loading levels than testing presented in (Weller et al., 2014b).

As discussed in Section 4.1, previous work has shown some stiffness dependency on both mean load and load amplitude for standard polyester ropes (Fernandes et al., 1999; Davies et al., 2002; Weller et al., 2014b, 2015b). Given the increase in mean load between the TCLL testing load levels it might be anticipated that an overall increase in stiffness would be observed between loading levels. However, due to a combination of the drop in stiffness due to adjustments between loading levels, the mild reduction in stiffness at the start of the 1–60% loading level, and the final failure occurring early in the 1–70% loading level, no such overall increase is observed. It is interesting to note however, that the significant increase in stiffness observed during the TCLL test series occurs in Phase 2 of operation as shown in Fig. 5 and Table 4, where the tether behaviour is dominated by the polyester rope as opposed to the EPDM core.

4.3. Marine exposure investigation

Results from ISO7743 testing conducted following a period of marine ageing demonstrate an average increase in sample stiffness of 15% and 22% for ACM and RCS respectively. To put these results into context within the range of EPDM Shore A hardness values specified in the P1 Series, Fig. 12 has been included. This figure demonstrates that although the ACM and RCS have increased following marine ageing, the change has not been significant enough to alter the order of the specified EPDM, with the aged 70.7 still having ACM and RCS values higher than for EPDM 70 and lower than EPDM 80.

There are various mechanisms which can contribute to changes in mechanical behaviour of elastomers after wet ageing: Reversible mechanisms include plasticization and swelling, irreversible effects include hydrolysis, leaching of additives such as plasticizers, and oxidation. These last two and possibly swelling will tend to result in increasing stiffness, while plasticization and hydrolysis may reduce it. More work including physico-chemical analysis is under way to identify the specific mechanisms which are involved here.

It should be noted that although establishing the value for ACM followed the standard ISO test procedure with a scaled sample size, the quantification of RCS is not a standard material test; the results for this are affected by both the material property and the sample geometry. This test was created specifically for the tether work presented, as the diametric compression behaviour of the EPDM cord is of critical importance to operation of the tether, controlling the axial stiffness profile during Phase 1 of operation. Thus the RCS result is not a standard material property that can be specified, but the presented work provides a better understanding of how this key property changes when the material is subject to realistic operating parameters.

Limitations of this work revolve around the assumption that immersing EPDM samples in heated sea water will accurately accelerate the natural ageing process in line with Arrhenius behaviour. Although this technique is widely used (Celina et al., 2005; Davies and Evrard, 2007; Le Saux et al., 2014; Le Gac et al., 2012; Scheirs, 2000; Wise et al.,

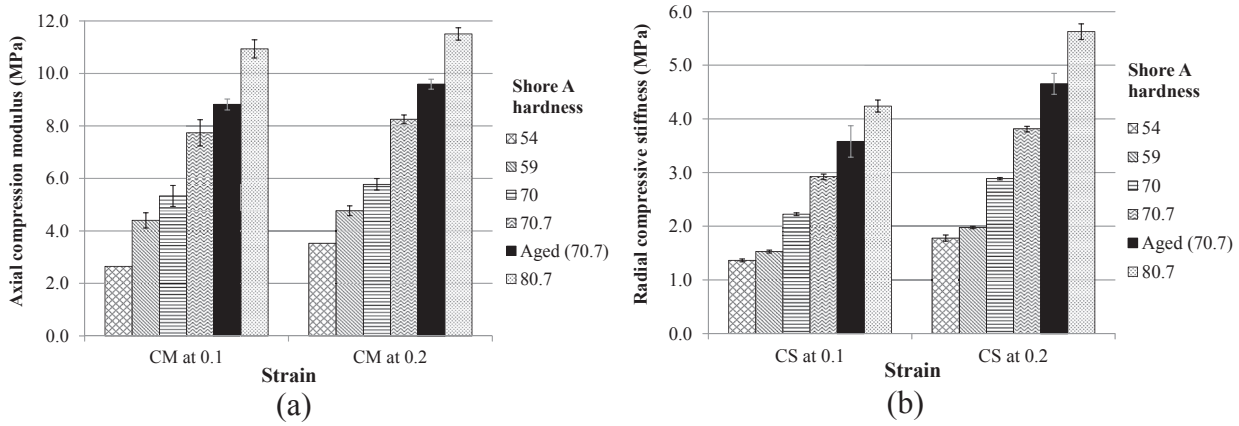

Fig. 12. Comparing the mean ACM (a) and RCS (b) values of aged EPDM to the original values calculated for the range of Shore A hardness virgin EPDM samples. The aged EPDM was aged for 13 months in renewed natural sea water at a temperature of 60 °C. Error bars based on sample standard deviation.

1995), it does have limitations, with critics concerned that using temperature to accelerate the ageing process may introduce failure mechanisms that would not have occurred through natural ageing at a more representative operational temperature (Davies and Evrard, 2007). The work presented here uses one temperature, 60 °C, to accelerate the marine ageing process, assuming that an Arrhenius relationship applies for EPDM. Given the apparent implications for the material properties of the EPDM samples tested, an extension to this work is underway to conduct further testing over a range of different temperatures to confirm these findings and to accurately establish the Arrhenius relationship for EPDM. Further to this, fatigue testing of samples in natural seawater will be conducted to establish the implications of concurrent exposure to fatigue cycling and the marine environment.

4.4. Radial compression fatigue investigation

The long term effect of the fatigue compression cycling is an average 15% increase in RCS, which was measured following 66 h of recovery. However, it is interesting to note that immediately after cycling the RCS is lower, gradually increasing and stabilising over time, with minimal change occurring between 42 and 66 h.

These compression test parameters represent a realistic, if conservative, loading scenario. Assembly tether testing observed radial compressive strains exceeding 0.35 during anticipated extreme conditions. Therefore exposing the EPDM cord to fatigue compression at a strain of 0.2 during this test schedule certainly represents a genuine operational demand. Further to this, assuming a typical wave period of 8 s, 707,000 cycles represent just 65 days of operation.

To put this observed change of RCS into context within the range of specified EPDM hardness values Fig. 13 has been included. This figure demonstrates that despite increasing the RCS of the material, the fatigued 70.7 EPDM remains in consecutive order of increasing RCS with increasing Shore A Hardness.

A potential limitation for this section of work revolves around the validity of these results due to the temperature increase of the samples when under compression cycling. To investigate this further detailed testing was conducted observing the temperature increase in samples when subjected to repeated compression cycles at a range of frequencies and to a varying degree of compressive strain. Measurable temperature increases were observed when subjecting samples to high frequency or high strain compression cycles. For example, at a strain of 0.2 and a frequency of 5 Hz, surface temperature increases peaking over 13 °C were observed. More significantly, at a strain of 0.5 and a frequency of 2 Hz surface temperature increases in excess of 35 °C were observed at the centre of the sample core cross section. The experimental parameters for the compression testing presented in this paper are based on a strain of 0.2 and a frequency of 2 Hz. Observed surface temperature differentials using these parameters remain below 9 °C and are therefore considered to have a minimal effect on results. This temperature increase may have affected the radial compressive stiffness calculated immediately following compression testing (Fig. 11) but should have limited effect on the longer term measured compressive stiffness values.

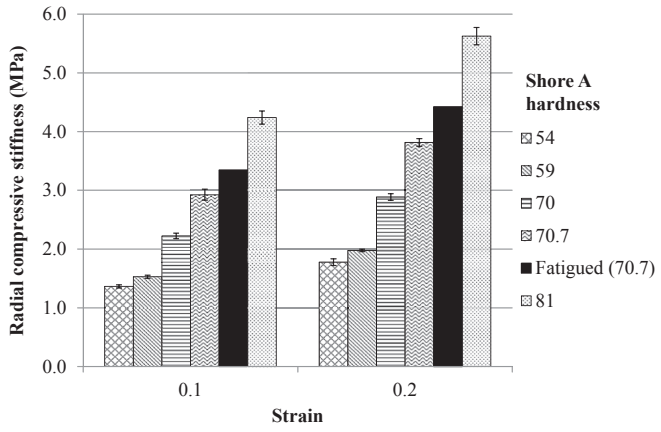

Fig. 13. Comparison of the stabilised RCS value of the fatigued EPDM sample with the original values calculated for the range of Shore A hardness virgin EPDM samples. The fatigued sample was subjected to 707,000 cycles of 0.2 compression strain at a frequency of 2 Hz. Presented results are based on the recovered sample 66h20 after the fatigue testing. Where used, error bars are based on sample standard deviation.

4.5. Overall discussion

Considering all these findings in the context of overall tether implications a pattern of increased stiffness when exposed to the marine environment and/or cyclical loading is established. Findings from the material tests are not directly comparable to the assembly scale tests however they do offer insights into what is causing the observed changes in tether assembly behaviour. The findings from the ISO7743 tests following either marine ageing or radial compression fatigue of the EPDM core material demonstrate an increased material resistance to compression. This supports the observed increase in tether stiffness during Phase 1 of tether operation following sea trials, where the core will have been subject to both the marine environment and radial compression fatigue.

To understand the relative contribution of different aspects of the material testing to the tether assembly performance, the ISO7743 material findings were plotted within the context of the range of hardness

values of the EPDM utilised in the P1 series prototype range in Figs. 12 and 13. These Figures demonstrate that, although significant, neither the marine ageing or radial compression fatigue testing shifted the order of the ACM or RCS across the range of EPDM Shore Hardness values tested. The conclusion from this is that there are multiple factors leading to the increase in stiffness observed in the aged tether assemblies following sea deployment. This includes changes to both the EPDM material radial compressive stiffness (caused by marine ageing and repeated radial compression of the core through the extension of the tether during operation), and the overall increase in stiffness of the polyester rope as observed in conventional polyester ropes (Bitting, 1980a; Bridon, 2017).

The work presented in this paper seeks to establish an understanding of the long term behaviour of the tether under typical operating parameters and does not address final failure mechanisms or fatigue failure rates. To establish a specific T-N curve for the tether would require a substantial test programme beyond the scope of work presented here and of limited use at this prototype stage. The polyester rope is the predominant load carrier within the tether and existing T-N curves for polyester rope (Flory and Banfield, 2006) can be used for fatigue estimation and design of mooring systems (Thies et al., 2014). The improved operating stiffness profile offered by the Exeter Tether will reduce both peak and fatigue loads throughout the mooring system, with (Parish et al., 2017) estimating a peak load reduction of approximately 70%. These load reductions should be considered when designing a floating system incorporating the tether as there are benefits that go beyond the mooring system, including a potential reduction in the required size of the floating body.

5. Conclusions and next steps

The P1-Series of tether prototypes were developed to prove the design concept of the Exeter Tether. The durability of this series was not a primary objective therefore the work presented in this paper offers some initial insights into key durability considerations for the P1 series in order to inform future design iterations.

Controlled testing of the tether assembly following a sea deployment approaching 6 months demonstrates a measurable increase in dynamic axial stiffness, with an average 82% and 8% increase in Phase 1 and 2 of operation respectively. Critically, this field deployment demonstrates that, for the two samples investigated, the diversity in stiffness profiles observed in the virgin tethers is reduced following a period of sea deployment. As the range of stiffness profiles is a key operating principle for the tether design, further work is required to establish if this reduction is observed across the full suite of tethers. Work is also ongoing utilising numerical models to estimate the load exposure of the tether prototypes during the SWMTF deployment and to establish the reduction in peak mooring loads achieved through tether placement within the mooring system.

The controlled assembly fatigue testing of tether P1-16 also highlighted the increase in dynamic axial stiffness upon working. The maximum increase of 42% was observed during the first loading level of 1–50% NWBS in the Phase 2 secant. This testing demonstrated the increase in stiffness stabilises over time reaching a natural limit. It is suggested that for each tether design a minimum of 500 cycles at typical operating loads is used to ascertain a working stiffness profile for use in mooring system design.

The dynamics of the floating system (and the resulting peak and fatigue mooring loads) will be significantly affected by the mooring stiffness profile. Establishing the ‘worked’ operating profiles of the tether assembly is of central importance to inform mooring systems designed to incorporate the tether.

In addition to tether assembly testing, detailed material tests of the EPDM core material established an increase in material stiffness when exposed to operational parameters including the marine environment and repeated compression cycles. Average increases in RCS of 22% and 15% were observed following marine ageing and exposure to fatigue compression cycles respectively. Prior to this work the effect of these parameters on EPDM was unknown. This information will therefore be useful to anyone intending to utilise EPDM in a marine environment or an application where it is repeatedly exposed to compressive strain.

Breaking the overall assembly down and conducting sub-component tests as presented in this paper allows a greater understanding of causality regarding the observed changes in the tether assembly operation. Going forward, it also creates an opportunity to investigate alternative materials more efficiently, without the need to construct full tether assemblies for each iteration.

This general approach, combining both field and laboratory experimentation to identify and investigate particular durability aspects of a novel component is particularly relevant for the offshore technology sector. Field work in this sector involves high operational costs, and although it is certainly necessary to prove components in the field, identifying opportunities for laboratory based testing to develop particular aspects of component investigation has shown to be an effective supplement to the field based work.

Bringing all aspects of the work presented here together, the assembly tether testing and EPDM material testing corroborate one another, all indicating an increased tether axial stiffness as a result of exposure to operating conditions. Marine ageing and low level loading (from the sea deployment) is found to significantly affect the stiffness during Phase 1 of tether operation, whilst high level fatigue loading has a greater impact on Phase 2 of the tether stiffness profile. The key objectives for the tether development are to increase the compliance of the mooring system and allow the specification of an axial stiffness optimised for a specific device and location. Whilst the tether successfully increases the overall compliance of the system as demonstrated in (Gordelier et al., 2015) and (Parish et al., 2017), this work has shown that the evolution of the tether stiffness profile during operation must be taken into account when designing a mooring system incorporating the Exeter Tether.

Following these findings, work has continued to further investigate the affect of marine ageing on EPDM. In addition, OPERA, a European Union Horizon 2020 project, has commissioned the development of upscaled tether prototypes including the P3 series and the full scale P4 series which will be deployed in the Bay of Biscay, Spain. The P4 tether will replace a conventional polyester rope on selected limbs of the Karratu shared mooring system, securing the MARMOK-A-5 wave energy device (Weller et al., 2017). Mooring load data from this deployment will allow an assessment of the load reductions achievable with this novel mooring system and a further assessment of the operational durability of the tether assembly.

Funding

This work was supported by the Engineering and Physical Sciences Research Council, via a PhD funded through the SuperGen UKCMER programme (Grant Numbers: EP/1027912/1 and EPN/M014738/1).

Additional funding was provided by the European Commission through the MARINET FP7 programme which funded access to the IFREMER Materials in a Marine Environment Laboratory for two weeks (Grant Number: 262552).

The P1 Tether series were developed with assistance from Lankhorst Ropes and HEFCE through the HE Innovation Fund.

The P3 and P4 Tether series were developed with Lankhorst Ropes as part of the OPERA Project, funded by the European Commission's Horizon 2020 programme under grant agreement No 654.444.

Data access statement

Due to the confidential nature of some of the research materials

supporting this publication not all of the data can be made accessible to other researchers. Please contact T.J.Gordelier@exeter.ac.uk for more information.

References

Bengtsson, N., Ekström, V., 2010. Seaflex. The Buoy Mooring System: Increase Life Cycle and Decrease Cost for Navigation Buoys. technical report, Tech. rep. https://doi.org/10.1016/j.oceaneng.2016.07.047.

Bitting, K.R., 1980a. The Dynamic Behavior of Nylon and Polyester Line. Coast Guard Research and Development Centre Groton CT (technical report No. CGR/DC-9/79). http://www.dtic.mil/get-tr-doc/pdf?AD=ADA087106.

Bitting, K.R., et al., 1980b. Cyclic tests of new and aged nylon and polyester line. In: Offshore Technology Conference, Offshore Technology Conference. https://doi.org/10.4043/3852-MS.

Bridon, 2017. Technical Information (online - last accessed 15/08/2017). http://www.bridon.com/uk/oil-and-gas-ropes/calm-buoy-off-take-mooring-systems/calm-buoy-off-take-mooring-system-ropes/viking-braidline-polyester/.

Cantournet, S., Desmorat, R., Besson, J., 2009. Mullins effect and cyclic stress softening of filled elastomers by internal sliding and friction thermodynamics model. Int. J. Solid Struct. 46 (11), 2255–2264. https://doi.org/10.1016/j.ijsolstr.2008.12.025.

Celina, M., Gillen, K., Assink, R., 2005. Accelerated aging and lifetime prediction: review of non-Arrhenius behaviour due to two competing processes. Polym. Degrad. Stabil. 90 (3), 395–404. https://doi.org/10.1016/j.polymdegradstab.2005.05.004.

Chailleux, E., Davies, P., 2005. A non-linear viscoelastic viscoplastic model for the behaviour of polyester fibres. Mech. Time-Dependent Mater. 9 (2), 147–160. https://doi.org/10.1007/s11043-005-1082-0.

Davies, P., Evrard, G., 2007. Accelerated ageing of polyurethanes for marine applications. Polym. Degrad. Stabil. 92 (8), 1455–1464. https://doi.org/10.1016/j.polymdegradstab.2007.05.016.

Davies, P., Huard, G., Grosjean, F., Francois, M., et al., 2000. Creep and relaxation of polyester mooring lines. In: Offshore Technology Conference, Offshore Technology Conference. https://doi.org/10.4043/12176-MS.

Davies, P., François, M., Grosjean, F., Baron, P., Salomon, K., Trassoudaine, D., et al., 2002. Synthetic mooring lines for depths to 3000 meters. Offshore Technology Conference, Offshore Technology Conference, Houston, Texas. https://doi.org/10.4043/14246-MS.

Davies, P., Weller, S., Johanning, L., 2012. Testing of Synthetic Fibre Ropes Deliverable 3.5.1., Tech. Rep. Deliverable 3.5.1 from the MERiFIC Project. MERiFIC. https://tinyurl.com/y8qsu9vr.

Davies, P., Johanning, L., Weller, S., Banfield, S., 2014. A review of sythetic fibre moorings for marine energy applications. In: International Conference on Ocean Energy, Halifax, Nova Scotia. http://archimer.ifremer.fr/doc/00251/36220/34771.pdf.

DeAndrade, O., Duggal, A., 2010. Analysis, design and installation of polyester rope mooring systems in deep water. In: Offshore Technology Conference, Houston, Paper OTC, vol. 20833.

Fernandes, A., Del Vecchio, C., Castro, G., et al., 1999. Mechanical properties of polyester mooring cables, Vol. 9. In: International Society of Offshore and Polar Engineers. https://www.onepetro.org/journal-paper/ISOPE-99-09-3-208.

Flory, J., Banfield, S.J., 2006. Durability of polyester ropes used as deepwater mooring lines. Oceans 1–5. https://doi.org/10.1109/OCEANS.2006.306947. Boston, USA, 18-21 September, IEEE.

Flory, J.F., Banfield, S.P., Petruska, D.J., 2004. Defining, measuring, and calculating the properties of fiber rope deepwater mooring lines. In: Offshore Technology Conference. https://doi.org/10.4043/16151-MS.

Gillen, K.T., Bernstein, R., Derzon, D.K., 2005. Evidence of non-Arrhenius behaviour from laboratory aging and 24-year field aging of polychloroprene rubber materials. Polym. Degrad. Stabil. 87 (1), 57–67. https://doi.org/10.1016/j.polymdegradstab.2004.06.010.

Gordelier, T., Parish, D., Thies, P.R., Johanning, L., 2015. A novel mooring tether for highly-dynamic offshore applications; mitigating peak and fatigue loads via selectable axial stiffness. J. Mar. Sci. Eng. 3 (4), 1287–1310. https://doi.org/10.1016/j.ijome.2014.06.001.

Harnois, V., Parish, D., Johanning, L., 17-19th October, 2012. Physical measurement of a slow drag of a drag embedment anchor during sea trials. In: 4th International Conference on Ocean Energy, Dublin. http://hdl.handle.net/10871/14399.

Harnois, V., Johanning, L., Thies, P., September, 2013. Wave conditions inducing extreme mooring loads on a dynamically responding moored structure. In: 10th EWTEC, Aalborg, Denmark. http://hdl.handle.net/10871/14303.

Harnois, V., Thies, P.R., Johanning, L., 2016. On peak mooring loads and the influence of environmental conditions for marine energy converters. J. Mar. Sci. Eng. 4 (2), 29. https://doi.org/10.3390/jmse4020029.

Harris, R., Johanning, L., Wolfram, J., 2004. Mooring systems for wave energy converters: a review of design issues and choices. In: 3rd International Conference on Marine Renewable Energy, Blyth UK.

ISO, 2004. Rubber, vulcanized or thermoplatic - estimation of life-time and maximum temperature of use. https://www.iso.org/standard/51795.html.

ISO, 2007. Fibre ropes for offshore stationkeeping - polyester, access via Cornwall online library system. https://www.iso.org/standard/38805.html.

ISO, 2011. Rubber, vulcanized or thermoplastic - determination of compression stress-strain properties. https://www.iso.org/standard/51795.html.

Johanning, L., Spargo, A., Parish, D., 2008. Large scale mooring test facility: a technical note. In: Proceedings of 2nd International Conference on Ocean Energy (ICOE).

Johanning, L., Thies, P., Smith, G., 2010. Component test facilities for marine renewable energy converters. In: Marine & Offshore Renewable Energy Conference paper 4. http://hdl.handle.net/10871/21105.

Le Gac, P.-Y., Le Saux, V., Paris, M., Marco, Y., 2012. Ageing mechanism and mechanical degradation behaviour of polychloroprene rubber in a marine environment: comparison of accelerated ageing and long term exposure. Polym. Degrad. Stabil. 97 (3), 288–296. https://doi.org/10.1016/j.polymdegradstab.2011.12.015.

Le Saux, V., Le Gac, P.-Y., Marco, Y., Calloch, S., 2014. Limits in the validity of Arrhenius predictions for field ageing of a silica filled polychloroprene in a marine environment. Polym. Degrad. Stabil. 99, 254–261. https://doi.org/10.1016/j.polymdegradstab.2013.10.027.

Low Carbon Innovation Coordination Group, August 2012. Technology innovation needs assessment (TINA): marine energy summary report, tech. Rep., low Carbon innovation coordination Group. https://www.carbontrust.com/media/168547/tina-marine-energy-summary-report.pdf.

Luxmoore, J.F., Grey, S., Newsam, D., Johanning, L., 2016. Analytical performance assessment of a novel active mooring system for load reduction in marine energy converters. Ocean Eng. 124, 215–225.

McEvoy, P., 2012. Combined elastomeric and thermoplastic mooring tethers. In: 4th International Conference on Ocean Energy, Dublin, Ireland.

McKenna, H., Hearle, J.W.S., O'Hear, N., 2000. Handbook of Fibre Rope Technology. Woodhead Publishing in Textiles, Cambridge, UK. https://tinyurl.com/ksh3wut.

Mueller, M., Wallace, R., 2008. Enabling science and technology for marine renewable energy. Energy Pol. 36 (12), 4376–4382. https://doi.org/10.1016/j.enpol.2008.09.035.

Oil Companies International Marine Forum, 2000. Guidelines for the Purchasing and Testing of SPM Hawsers. Witherby's Publishing, Livingston, UK.

Parish, D., Johanning, L., 2012. Mooring Limb. US Patent Application Pub. No. US 2012/0298028 A1. http://www.google.com/patents/US20120298028.

Parish, D., Herduin, M., Gordelier, T., Thies, P., Johanning, L., 2017. Reducing peak and fatigue mooring loads: a validation study for elastomeric moorings. In: European Wave and Tidal Energy Conference Series, 27 August - 1 September, Cork, Ireland. http://hdl.handle.net/10871/29126.

Ridge, I., Banfield, S., Mackay, J., 2010. Nylon fibre rope moorings for wave energy converters. Oceans. https://doi.org/10.1109/OCEANS.2010.5663836.

Salter, S., 2003. Research requirements for fourth generation wave energy devices. Results from the work of the European Thematic Network in Wave Energy, Tech. rep., 58. University of Edinburgh. paper.

Scheirs, J., 2000. Compositional and Failure Analysis of Polymers: a Practical Approach. John Wiley & Sons.

Thies, P., Johanning, L., Harnois, V., Smith, H., Parish, D., 2014. Mooring line fatigue damage evaluation for floating marine energy converters: field measruements and prediction. Renew. Energy 63, 133–144. https://doi.org/10.1016/j.renene.2013.08.050.

Thies, P., Crowley, S., Johanning, L., Micklethwaite, W., Ye, H., Tang, D., Cui, L., Li, X., 2015. Novel mooring design options for high-intensity typhoon conditions - an investigation for wave energy in China. In: RINA Structural Load and Fatigue on Floating Structures Conference, 25 February, London, UK, 2015. http://hdl.handle.net/10871/17665.

Weller, S., Hardwick, J., Johanning, L., Karimirad, M., Teillant, B., Raventos, A., Banfield, S., Delaney, M., Yeats, B., Sheng, W., 2014a. Deliverable 4.1: a comprehensive assessment of the applicability of available and proposed offshore mooring and foundation technologies and design tools for array applications. http://hdl.handle.net/10871/23587.

Weller, S., Davies, P., Vickers, A., Johanning, L., 2014b. Synthetic rope responses in the context of load history: operational performance. Ocean Eng. 83, 111–124. https://doi.org/10.1016/j.oceaneng.2014.03.010.

Weller, S., Johanning, L., Davies, P., Banfield, S., 2015a. Synthetic mooring ropes for marine renewable energy applications. Renew. Energy 83, 1268–1278.

Weller, S., Davies, P., Vickers, A., Johanning, L., 2015b. Synthetic rope responses in the context of load history: the influence of aging. Ocean Eng. 96, 192–204. https://doi.org/10.1016/j.oceaneng.2014.12.013.

Weller, S., Parish, D., Gordelier, T., Migeul Para, B. d., Garcia, E., Goodwin, P., Tornroos, D., Johanning, L., 2017. Open sea OWC motions and mooring loads monitoring at BiMEP. In: European Wave and Tidal Energy Conference Series, Cork, Ireland.

Wise, J., Gillen, K., Clough, R., 1995. An ultrasensitive technique for testing the Arrhenius extrapolation assumption for thermally aged elastomers. Polym. Degrad. Stabil. 49 (3), 403–418. https://doi.org/10.1016/0141-3910(95)00137-B.